

SUPPLEMENTARY INFORMATION

Hypothalamic AMPK and fatty acid metabolism mediate thyroid regulation of energy balance

Miguel López^{1,2,3}, Luis Varela^{1,2}, María J. Vázquez^{1,2},
Sergio Rodríguez-Cuenca³, Carmen R. González^{1,2}, Vidya R. Velagapudi⁴,
Donald A. Morgan⁵, Erik Schoenmakers³, Khristofor Agassandian⁶,
Ricardo Lage^{1,2}, Pablo Blanco Martínez de Morentin^{1,2}, Sulay Tovar^{1,2},
Rubén Nogueiras^{1,2}, David Carling⁷, Christopher Lelliott⁸,
Rosalía Gallego^{9,11}, Matej Orešič^{4,11}, Krishna Chatterjee^{3,11}, Asish K. Saha^{10,11},
Kamal Rahmouni⁵, Carlos Diéguez^{1,2} & Antonio Vidal-Puig³

¹ Department of Physiology, School of Medicine, University of Santiago de Compostela-Instituto de Investigación Sanitaria, Santiago de Compostela (A Coruña), 15782, Spain

² CIBER Fisiopatología de la Obesidad y Nutrición (CIBERObn), 15706, Spain

³ Institute of Metabolic Science, Metabolic Research Laboratories, Addenbrooke's Hospital, University of Cambridge, Cambridge, CB2 0QQ, UK

⁴ VTT Technical Research Centre of Finland, Tietotie 2, Espoo, FIN-02044, Finland

^{5, 6} Departments of ⁵Internal Medicine and ⁶Anatomy and Cell Biology, University of Iowa Carver College of Medicine, Iowa City, Iowa, 52242, USA

⁷ Cellular Stress Group, Medical Research Council Clinical Sciences Centre, Hammersmith Hospital, Imperial College, London, W12 0NN, UK

⁸ Department of Biosciences, AstraZeneca R&D, Mölndal, S-43183, Sweden

⁹ Department of Morphological Sciences, School of Medicine, University of Santiago de Compostela, 15782, Spain

¹⁰ Diabetes Research Unit, EBRC-827, Boston Medical Center, Boston, MA 02118, USA

¹¹ These authors contributed equally to this work

Correspondence should be addressed to: M.L. (m.lopez@usc.es) or A.V-P. (ajv22@cam.ac.uk)

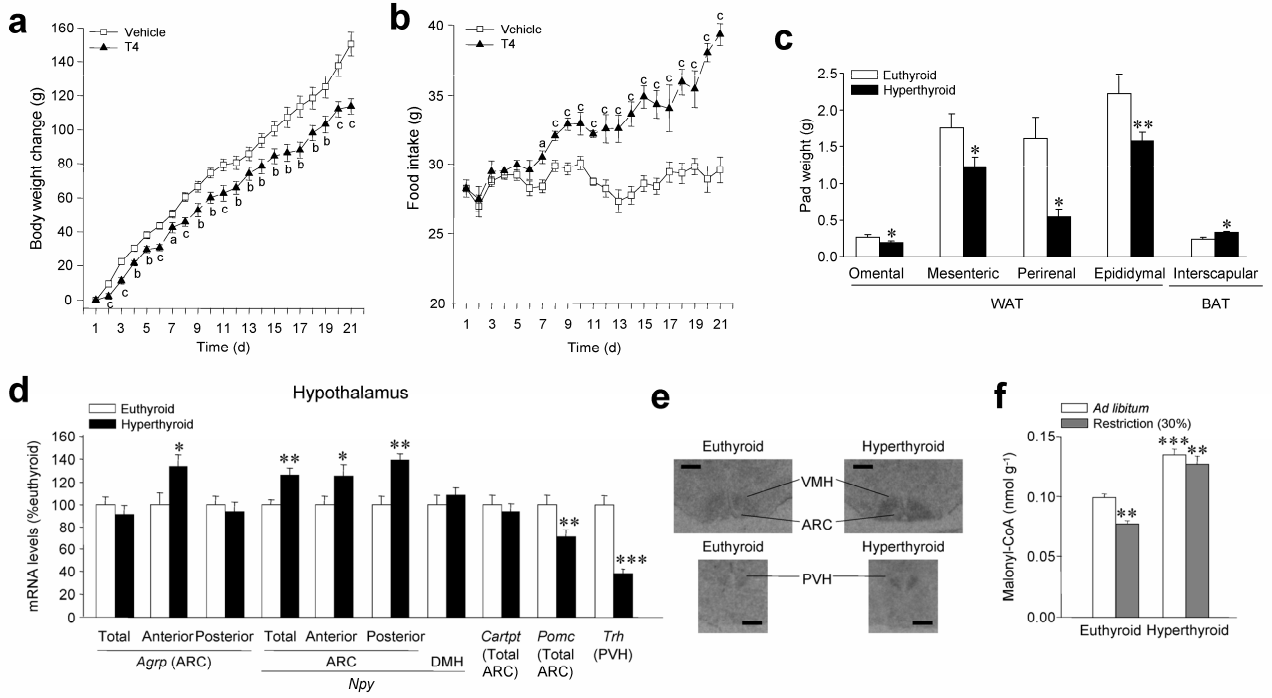
Supplementary Table 1: Body and plasma parameters and hypothalamic (PVH) TRH levels of euthyroid, hyperthyroid and hypothyroid rats

| | Euthyroid | Hyperthyroid | Hypothyroid |
|---|------------------|---------------------|--------------------|
| Body length (cm, with tail) | 44.44±0.18 | 44.25±0.25 | 42.63±0.46** |
| Body length (cm, without tail) | 24.78±0.22 | 24.50±0.29 | 23.75±0.25** |
| Fat mass (g) | 34.99±2.06 | 17.25±1.90 *** | - |
| Non-fat mass (g) | 314.61 ±5.84 | 295.83±5.29** | - |
| Free water (g) | 1.32±0.09 | 1.19±0.08 | - |
| Temperature (°C) | 34.60±0.09 | 35.43±0.13*** | - |
| Food efficiency (g Kcal ⁻¹) | 0.19±0.01 | 0.12±0.01*** | - |
| TSH (ng ml ⁻¹) | 3.47±0.20 | 0.42 ± 0.08*** | 27.17±1.71*** |
| T4 (nmol l ⁻¹) | 80.20±7.16 | 321.64±33.42*** | 25.0±7.67*** |
| T3 (nmol l ⁻¹) | 3.17±0.23 | 5.10±0.64*** | 1.28±0.19*** |
| Glucose (mmol l ⁻¹) | 7.36±0.15 | 7.38±0.35 | 6.12±0.23* |
| Insulin (ng ml ⁻¹) | 2.11±0.34 | 2.48±0.41 | 1.50±0.55 |
| Leptin (ng ml ⁻¹) | 3.89±0.46 | 1.65±0.42*** | 3.40±1.05 |
| <i>Trh</i> PVH (% euthyroid) | 100.00±9.29 | 40.15±4.51*** | 189.68±14.45*** |

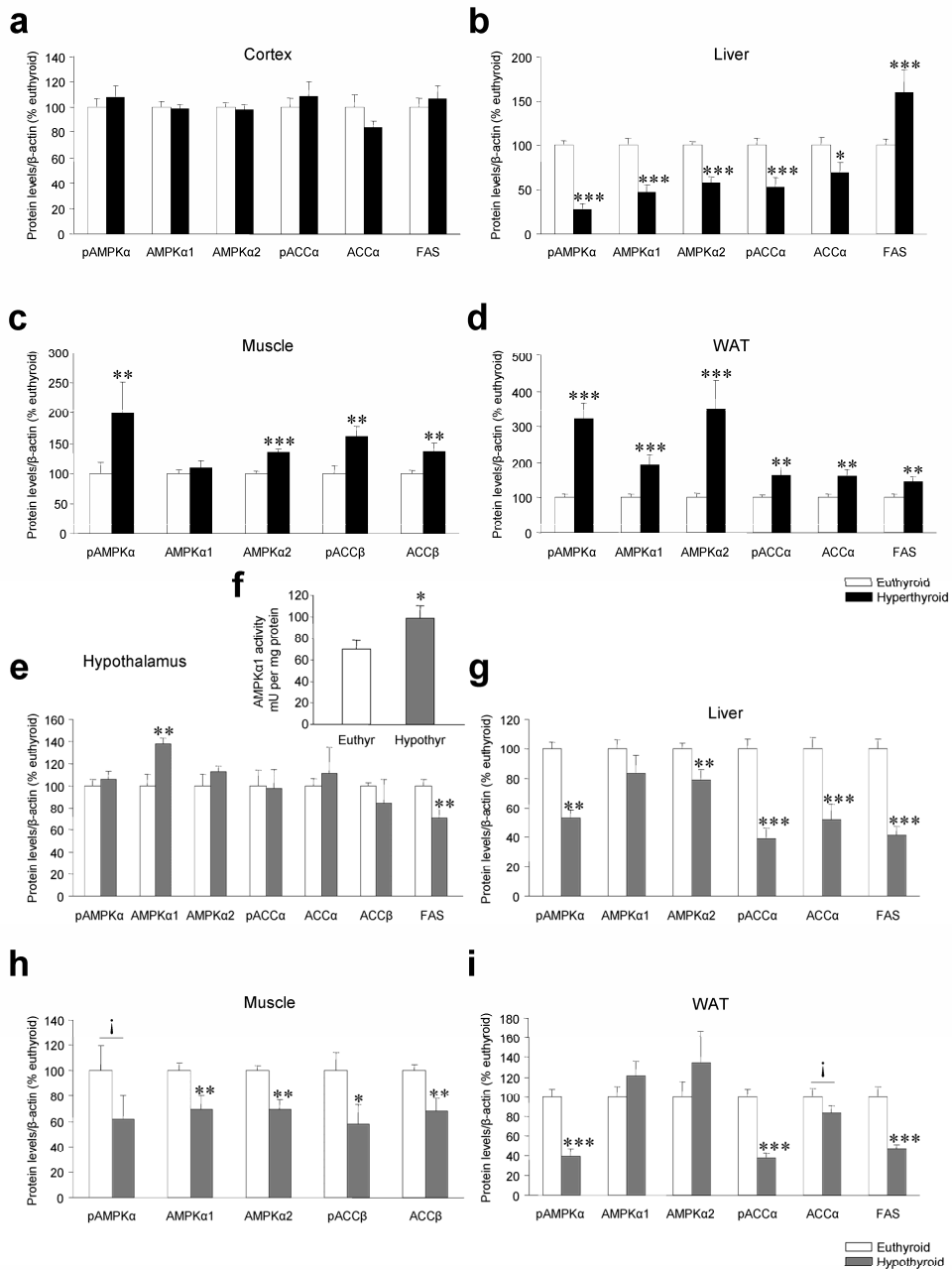
* : P<0.05 vs. Euthyroid

** : P<0.01 vs. Euthyroid

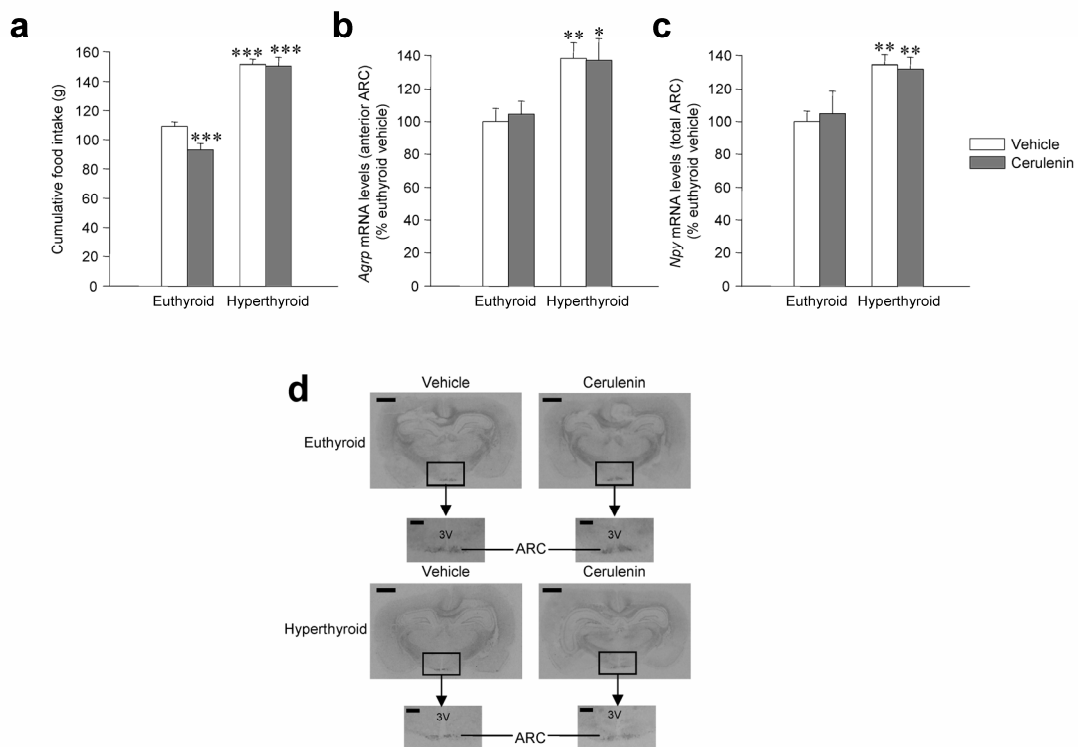
***: P<0.001 vs. Euthyroid



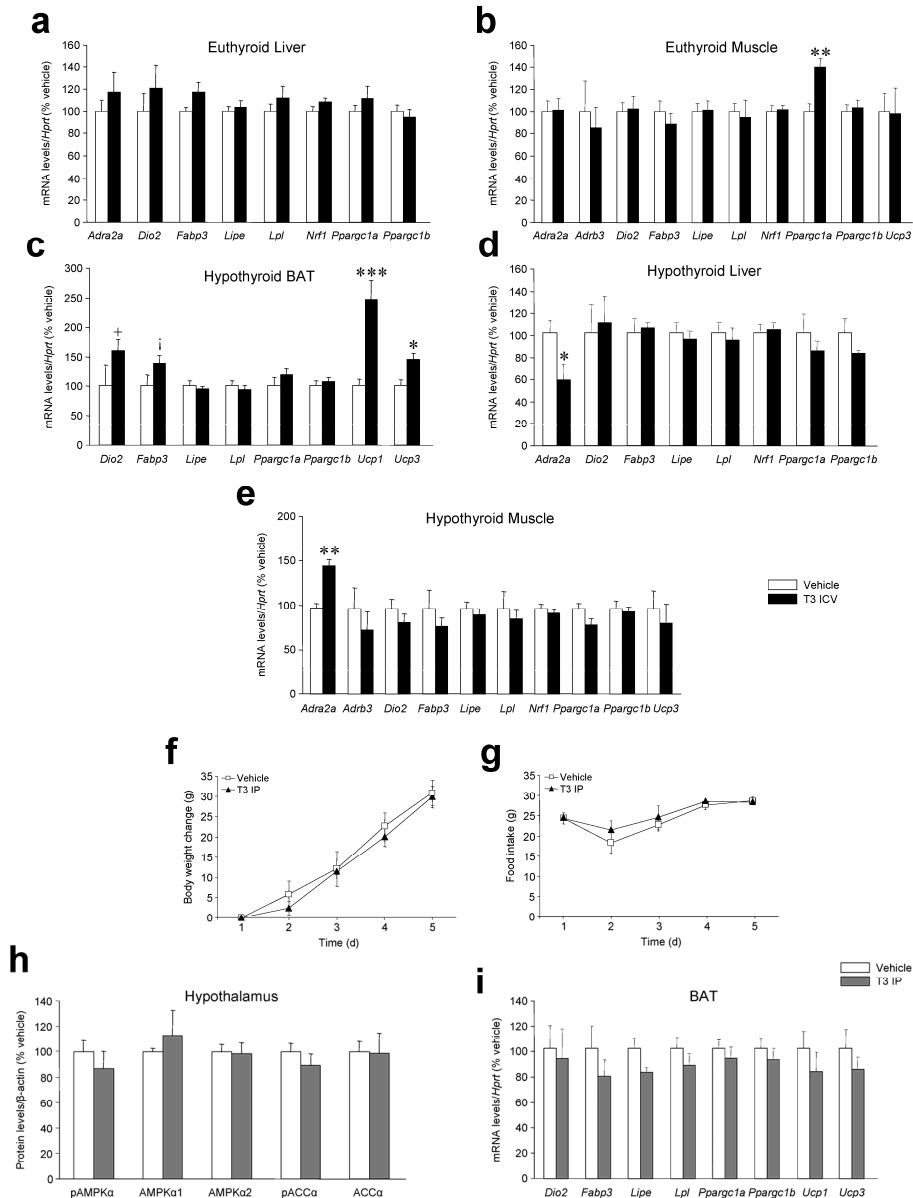
Supplementary Figure 1. Energy balance and hypothalamic parameters in hyperthyroid rats. (a) Body weight change, (b) daily food intake, (c) weights of fat pads, (d) hypothalamic neuropeptide mRNA expression, (e) in situ hybridization images (scale bar, 500 μ m) showing *Fasn* mRNA expression and (f) hypothalamic malonyl-CoA response to food restriction of euthyroid and hyperthyroid rats. * or "a" $P < 0.05$, ** or "b" $P < 0.01$, *** or "c" : $P < 0.001$ vs. vehicle or euthyroid; all data are expressed as mean \pm SEM. *Cartpt*: gene encoding CART (cocaine and amphetamine-regulated transcript).



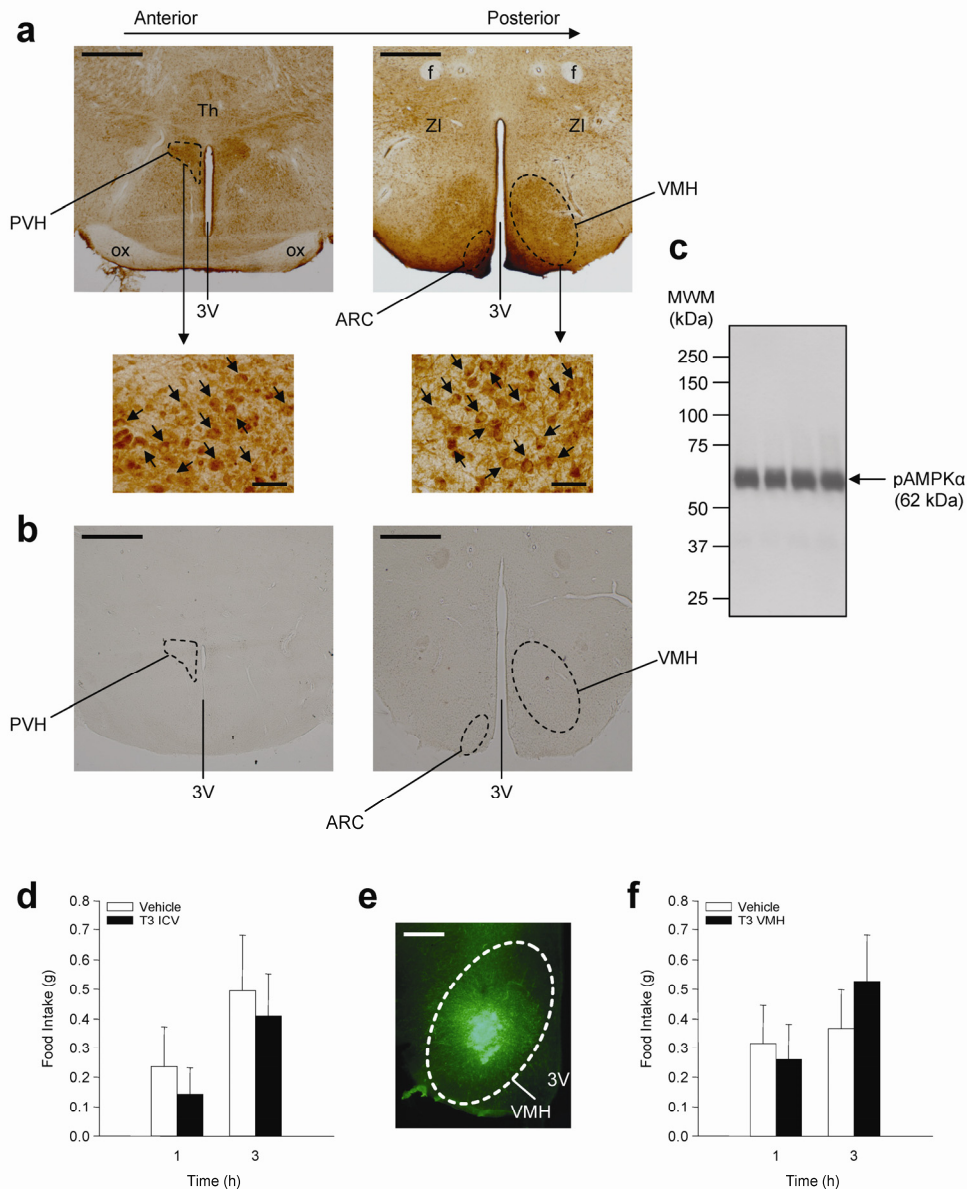
Supplementary Figure 2. Regulation of AMPK pathway in hyperthyroid and hypothyroid rats. (a–d) Protein levels of pAMPK α , AMPK α 1, AMPK α 2, pACC α , ACC α , and FAS in the brain cortex (a), liver (b), muscle (c) and WAT (d) of euthyroid and hyperthyroid rats. **(e–i)** Protein levels of pAMPK α , AMPK α 1, AMPK α 2, pACC α (or pACC β in muscle), ACC α (or ACC β in muscle) and FAS and AMPK α 1 activity in the hypothalamus (e, f), liver (g), muscle (h) and WAT (i) of euthyroid and hypothyroid rats. $iP = 0.08$, $*P < 0.05$, $**P < 0.01$, $***P < 0.001$ vs. euthyroid; all data are expressed as mean \pm SEM.



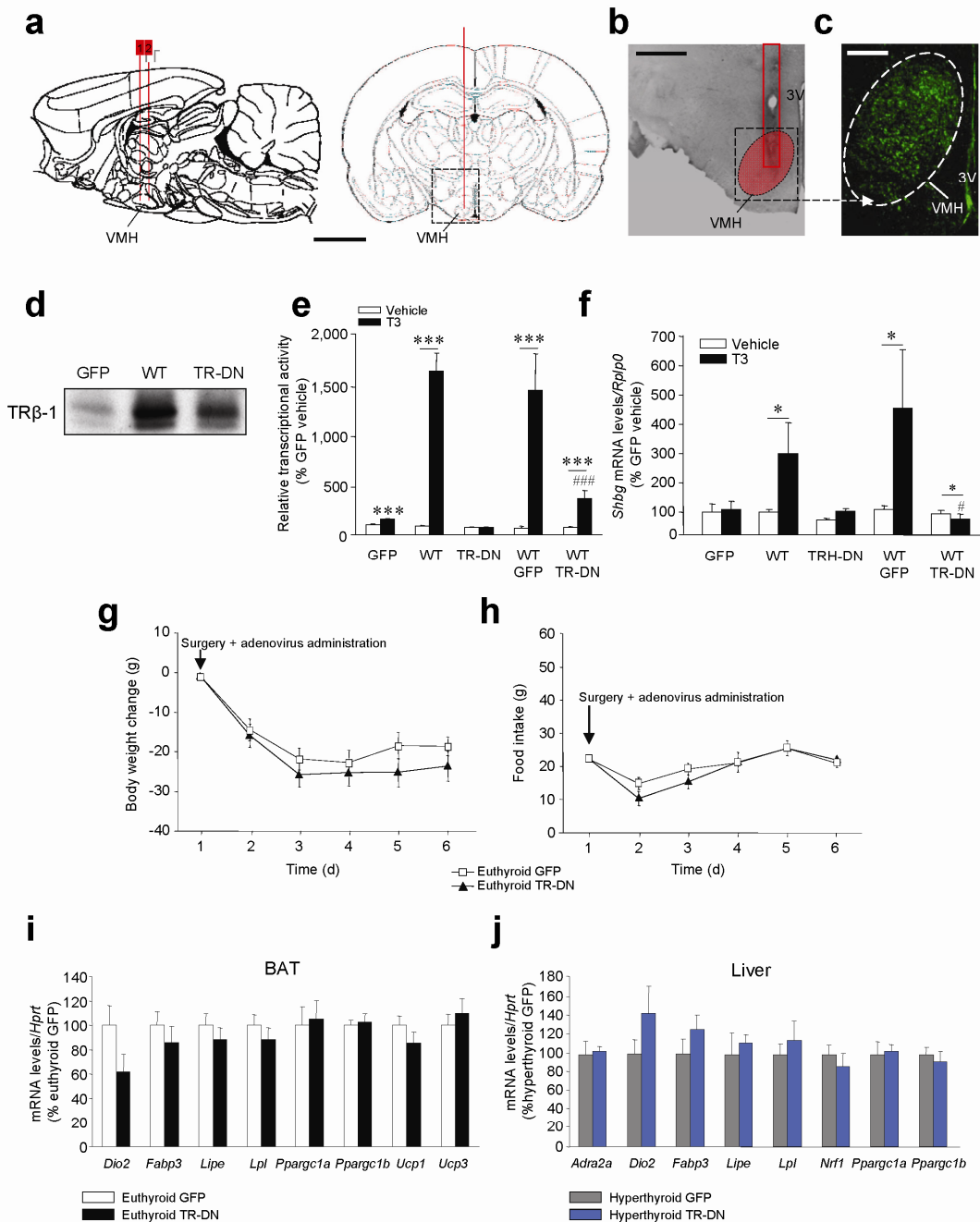
Supplementary Figure 3. Food intake and neuropeptide changes induced by central inhibition of FAS. (a) Cumulative food intake, (b) *Agrp* mRNA levels in the anterior ARC, (c) *Npy* levels in the total ARC and (d) in situ hybridization images (upper images: scale bar, 2 mm; lower images, scale bar, 500 μ m) showing *Pomc* mRNA levels in the total ARC of euthyroid and hyperthyroid rats ICV-treated with cerulenin. * $P < 0.05$, ** $P < 0.01$, *** $P < 0.001$ vs. euthyroid vehicle; all data are expressed as mean \pm SEM.



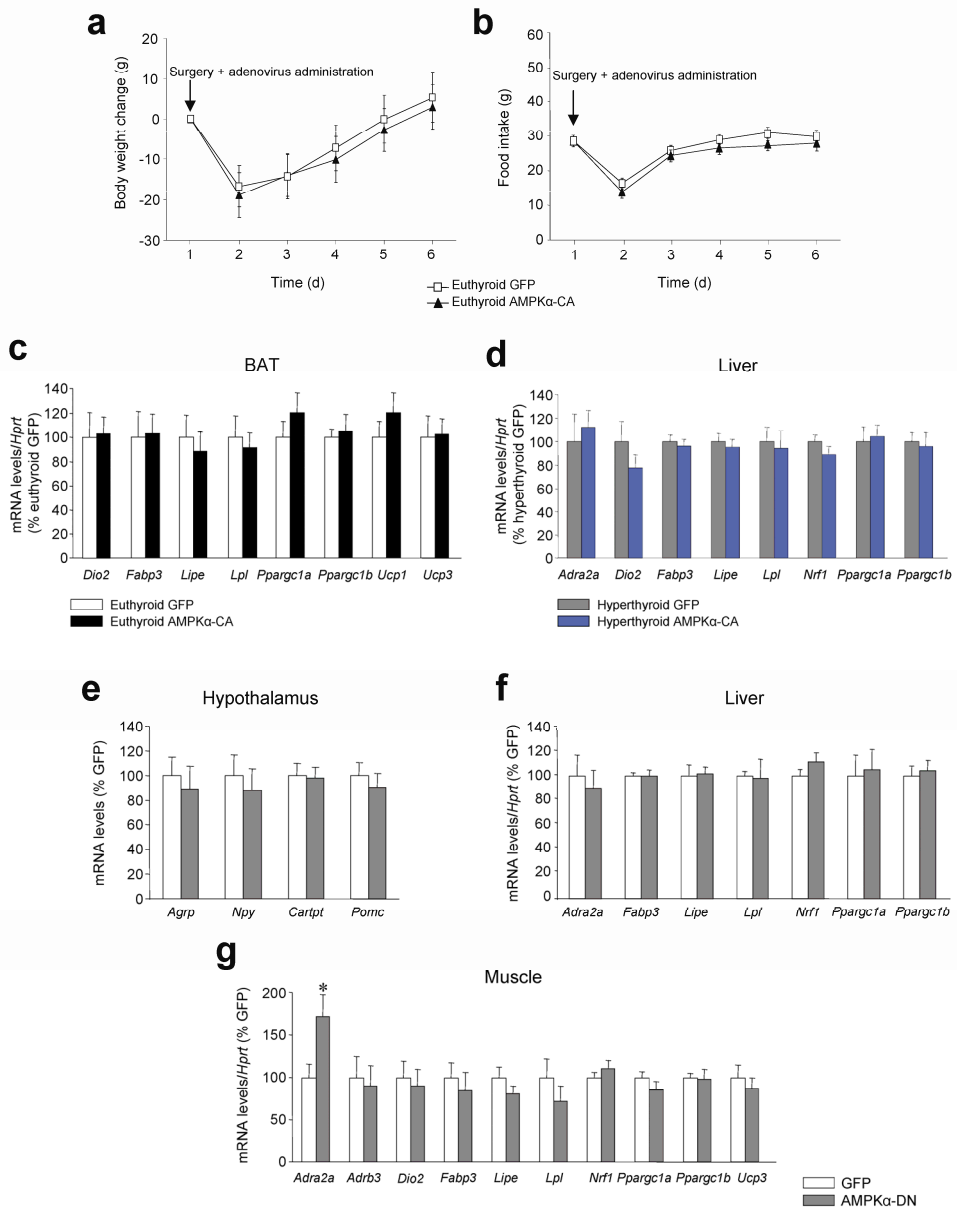
Supplementary Figure 4. Molecular and physiological effects of chronic central T3 administration. (a–b) mRNA expression profiles in the liver (a) and muscle (b) of euthyroid rats ICV-treated with T3 for 4 d. (c–e) mRNA expression profiles in the BAT (c), liver (d) and muscle (e) of hypothyroid rats ICV-treated with T3 for 4 d. (f–i) Body weight gain (f), daily food intake (g), hypothalamic pAMPKα, AMPKα1, AMPKα2, pACCα and ACCα protein levels (h) and mRNA expression profiles in the BAT (i) of euthyroid rats IP-treated with T3 for 4 d. $jP = 0.08$, $+P = 0.06$, $*P < 0.05$, $**P < 0.01$, $***P < 0.001$ vs. vehicle; all data are expressed as mean \pm SEM. *Adra2a*: gene encoding $\alpha 2A$ -AR (adrenergic receptor alpha 2a); *Nrf1*: gene encoding NRF-1 (nuclear respiratory factor 1).



Supplementary Figure 5. Molecular and physiological effects of central T3 action in the hypothalamus. (a–c) Hypothalamic pAMPK α immunoreactivity (IR) (upper 40 \times , scale bar 500 μ m; lower: 200 \times , scale bar, 20 μ m), the dotted lines show the ARC, the PVH and the VMH (a). Pre-absorption with control peptide showing lack of positive pAMPK α -IR (40 \times , scale bar 500 μ m) (b). Western blot showing the specificity of anti-pAMPK α -Thr172 antibody on hypothalamic protein extracts. The antibody just detected pAMPK α at the expected molecular weight (62 kDa) and no additional bands were observed (c). (d) Food intake of euthyroid rats treated with T3 ICV. (e–f) Immunofluorescence (40 \times , scale bar, 200 μ m) showing the presence of the dye (fluorescein isothiocyanate dextran 7000) after co-microinjection with T3 into the VMH (e) and food intake of euthyroid rats treated with T3 stereotaxically into the VMH (f). All data are expressed as mean \pm SEM. 3V: third ventricle; Th: thalamus; ox: optic chiasm; ZI: zona incerta (thalamus).



Supplementary Figure 6. Genetic ablation of thyroid hormone receptor in the VMH. (a–c) Localization studies (scale bar, 2 mm) showing the injection route for stereotaxic microinjections of adenoviral expression vectors into the VMH. Two injections (labeled as 1 and 2) were given in each VMH (scale bar, 2 mm) (a). The injection route enclosed in a red rectangle is precisely placed in the VMH (10 ×, scale bar, 500 μm) (b). Representative immunofluorescence (40 ×, scale bar, 200 μm) with anti-GFP antibody showing GFP expression in the VMH of rats treated with adenoviruses (c). (d) Western blot for protein levels of TRβ-1 in adenoviruses-infected HepG2 cells. (e) Transcriptional activity of a thyroid hormone response element containing reporter gene without or with 100 nM T3 in HepG2 cells, infected with control (GFP), wildtype (WT) or mutant thyroid hormone receptor dominant negative (TR-DN) expressing adenoviruses. (f) Expression of an endogenous target gene (*Shbg*) without or with 100 nM T3 in HepG2 cells, infected with control (GFP), wild type (WT) or mutant thyroid hormone receptor dominant negative (TR-DN) expressing adenoviruses. (g–j) Body weight change (g), daily food intake (h) and mRNA expression profiles in BAT of euthyroid rats (i) and liver of hyperthyroid rats (j) stereotaxically treated with a GFP-expressing adenoviruses or GFP plus TR-DN adenoviruses into the VMH. * $P < 0.05$, *** $P < 0.001$ vs. vehicle; # $P < 0.05$ WT TR-DN T3 vs. WT T3 and WT GFP T3; #### $P < 0.001$ WT TR-DN T3 vs. WT T3 and WT GFP T3; all data are expressed as mean ± SEM.



Supplementary Figure 7. Molecular and physiological effects of administration of AMPK-CA or AMPK-DN adenovirus in the VMH. (a–d) Body weight change (a), daily food intake (b) and mRNA expression profiles in BAT of euthyroid rats (c) and in liver of hyperthyroid rats (d) stereotactically treated with a GFP-expressing adenoviruses or GFP plus AMPK α -CA adenoviruses into the VMH. (e–g) Hypothalamic neuropeptide mRNA expression (e), mRNA expression profiles in liver (f) and muscle (g) of euthyroid rats stereotactically treated with adenoviruses expressing GFP or GFP plus AMPK-DN into the VMH. * $P < 0.05$ vs. GFP. All data are expressed as mean \pm SEM.

SUPPLEMENTARY METHODS

Animals and sample preparation. We used adult male Sprague-Dawley rats (9–11 weeks old, *Animalario General USC*; and *Harlan Sprague-Dawley*). USC and University of Iowa Animal Research Committees approved all procedures. All studies were conducted in accordance with the International Law on Animal Experimentation and National Institutes of Health (NIH) Guide for the Care and Use of Laboratory Animals. For all the experimental groups and analytic methods, we use 9–12 rats per group as a minimum. All the experiments were repeated at least twice. Rats were killed by cervical dislocation and quickly decapitated, in a separate room, and their tissues (brain, liver, BAT, WAT and muscle) removed. For hypothalamic studies, one set of brains animals per experimental group was removed intact for *in situ* hybridization analysis, when required. In another set of brains the hypothalamus was dissected, as previously described^{1–5} for protein and activity or metabolite determination. All these samples were frozen immediately on dry ice and maintained at – 80 °C until processed. We collected trunk blood in heparinized tubes, centrifuged immediately, separated the plasma and kept frozen at – 20 °C until assayed. For immunohistochemical techniques rats were deeply anaesthetized with ketamine and xylazine and then fixed by perfusion using formaline. Brains were removed and immersed for 2–4 h in the same fixative followed by a washing step in phosphate buffer 0.1M for 1 h. Fifty- μ m vibratome sections were processed for immunohistochemical and double immunofluorescence free floating methods, as previously shown (see below)^{2,6}.

Stereotaxic microinjection of adenoviral expression vectors and T3 microinjections. We placed rats in a stereotaxic frame (*David Kopf Instruments*) under ketamine-xylazine

anesthesia. The VMH was targeted bilaterally as previously reported². Adenoviruses vectors (*Viraquest*; North Liberty) either 1) GFP (1×10^{12} pfu ml⁻¹, control adenoviruses) or 2) GFP plus AMPK α dominant negative (AMPK α -DN; 1×10^{12} pfu ml⁻¹), or 3) GFP plus AMPK α constitutively active (AMPK α -CA; 2×10^{10} pfu ml⁻¹), or 4) GFP plus thyroid hormone receptor dominant negative (TR-DN; 3×10^{10} pfu ml⁻¹) were delivered at a rate of 200 nl min⁻¹ for 5 min (1 μ l per injection site)². For the VMH microinjections, T3 (0.4 ng in 100 nl of DMSO) or vehicle (100 nl of DMSO) was given; the pipette was left in place for 5–10 min and then removed. We performed measurements after 1 h for the hypothalamic protein studies and during 6 h for the BAT SNA experiments. We mixed fluorescent dye (fluorescein isothiocyanate dextran 7000; *Sigma*) with T3 and vehicle for each injection to assess the accuracy of the injection site. Only animals that showed VMH-specific location of the injections (dye) were included (**Supplementary Fig. 5e**).

Sympathetic nerve activity recording. We anesthetized rats using intraperitoneal ketamine (91 mg kg⁻¹) and xylazine (9.1 mg kg⁻¹) and maintained anesthesia with α -chloralose (initial dose: 25mg kg⁻¹, sustain dose: 50 mg kg⁻¹ h⁻¹) via a catheter inserted in the femoral vein. The trachea was cannulated, and each rat was allowed to breathe spontaneously oxygen-enriched air. Rectal temperature was maintained at 37.5°C using a temperature-controlled surgical table and a lamp. We obtained multi-fiber recording of SNA from the nerve subserving BAT, as previously described^{7,8}. Using a dissecting microscope, a nerve fiber innervating interscapular BAT was identified, placed on the bipolar platinum-iridium electrode. Each electrode was attached to a high-impedance probe (HIP-511, *Grass Instruments*) and the nerve signal was amplified 10⁵ times with a Grass P5 AC pre-amplifier. After amplification, the nerve signal was filtered at a 100- and 1000-Hz cutoff with a nerve traffic analysis system (Model 706C, *University of Iowa Bioengineering*). The nerve signal was then routed to an oscilloscope

(model 54501A, *Hewlett-Packard*) for monitoring the quality of the sympathetic nerve recording and to a resetting voltage integrator (model B600c, *University of Iowa Bioengineering*). BAT SNA measurements were made every 15 min for 6 h after ICV and VMH microinjections. To ensure that electrical noise was excluded in the assessment of sympathetic outflow, we corrected each SNA recording for post-mortem background activity

Blood biochemistry. We measured Plasma TSH, T3, T4, leptin and insulin using rat ELISA kits (*Crystal Chem Inc*). Kits for the measurement of glucose were obtained from *Roche*.

Real-time quantitative PCR. We performed real-time PCR (TaqMan®; Applied Biosystems) as previously described ^{1, 3, 6, 8}, using the following sets of primers and probes (*GenBank* accession number is inside brackets after gene's name):

Adra2a (NM_012739): gene encoding adrenergic receptor alpha 2a (α 2A-AR)

Forward primer: 5'-GGTGGTGATCGGCGTGTT-3'

Reverse primer: 5'-CGACGGCTATGAGCGTGTA-3'

Probe: FAM-5'-TGGTGTGTTGGTTCCCGTTCTTTTCA-3'-TAMRA

Adrb3 (NM_013108): gene encoding adrenergic receptor beta 3 (β 3-AR)

Forward primer: 5'-CCTTCCCAGCTAGCCCTGTT-3'

Reverse primer: 5'-TGCTAGATCTCCATGGTCCTTCA-3'

Probe: FAM-5'-AACTCACCGCTCAACAGGTTTGATGGC-3'-TAMRA

Dio2 (NM_031720): gene encoding type 2 deiodinase (D2)

Applied Biosystems TaqMan® Expression Assays; Assay ID Rn00581867_m1

Fabp3 (NM_024162): gene encoding fatty acid binding protein 3 (FABP3)

Forward primer: 5'-ACGGAGGCAAACCTGGTCCAT-3'

Reverse primer: 5'-CACTTAGTTCCCGTGTAAGCGTAGTC-3'

Probe: FAM-5'-TGCAGAAGTGGGACGGGCAGG-3'-TAMRA

Hprt (NM_012583): gene encoding hypoxanthine guanine phosphoribosyl transferase (HPRT)

Forward primer: 5'-AGCCGACCGGTTCTGTCAT-3'

Reverse primer: 5'-GGTCATAACCTGGTTCATCATCAC -3'

Probe: FAM-5'-CGACCCTCAGTCCCAGCGTCGTGAT 3'-TAMRA

Lipe (NM_012859): gene encoding hormone sensitive lipase (HSL)

Forward primer: 5'-CCAAGTGTGTGAGCGCCTATT -3'

Reverse primer: 5'-TCACGCCCAATGCCTTCT -3'

Probe: FAM-5'-AGGGACAGAGACGGAGGACCATTTTGACTC -3'-TAMRA

Lpl (NM_012598): gene encoding lipoprotein lipase (LPL)

Forward primer: 5'-CTGAAAGTGAGAACATTCCCTTCA-3'

Reverse primer: 5'-CCGTGTAAATCAAGAAGGAGTAGGTT-3'

Probe: FAM-5'-CCTGCCGGAGGTCGCCACAAATA-3'-TAMRA

Nrf1 (NM_001100708): gene encoding nuclear respiratory factor 1 (NRF1)

Forward primer: 5'-TGTTTGGCGCAGCACCTTT-3'

Reverse primer: 5'-CGCAGACTCCAGGTCTTCCA-3'

Probe: FAM-5'-ATGTGGTGCGCAAGTACAAGAGCATGATC-3'-TAMRA

Ppargc1a (NM_031347): gene encoding peroxisome-proliferator-activated receptor-gamma co-activator 1 alpha (PGC1 α)

Forward primer: 5'-CGATCACCATATTCCAGGTCAAG-3'

Reverse primer: 5'-CGATGTGTGCGGTGTCTGTAGT -3'

Probe: FAM-5'-AGGTCCCCAGGCAGTAGATCCTCTTCAAGA-3'-TAMRA

Ppargc1b (NM_176075): gene encoding peroxisome-proliferator-activated receptor-gamma co-activator 1 beta (PGC1 β)

Applied Biosystems TaqMan® Expression Assays; Assay ID Rn00598552_m1

Rplp0 (NM_001002): gene encoding ribosomal protein, large, P0 (RPLP0)

Forward primer: 5'-AGATGCAGCAGATCCGCAT-3'

Reverse primer: 5'-ATATGAGGCAGCAGTTTCTCCAG-3'

Probe: FAM-5'-AGGCTGTGGTGCTGATGGGCAAGAA-3'-TAMRA

Shbg (NM_001040): gene encoding sex hormone binding globulin (SHBG)

Applied Biosystems TaqMan® Expression Assays; Assay ID HS00168927_m1

Ucp1 (NM_012682): gene encoding uncoupling protein 1 (UCP1)

Forward primer: 5'-CAATGACCATGTACACCAAGGAA-3'

Reverse primer: 5'-GATCCGAGTCGCAGAAAAGAA-3'

Probe: FAM-5'-ACCGGCAGCCTTTTTCAAAGGGTTTG-3'-TAMRA

Ucp3 (NM_013167): gene encoding uncoupling protein 1 (UCP3)

Applied Biosystems TaqMan® Expression Assays; Assay ID Rn00565874_m1

In situ hybridization. Coronal hypothalamic sections (16 μ m) were cut on a cryostat and immediately stored at -80°C until hybridization. We used specific oligos for AgRP, CART, FAS, NPY, POMC and TRH detection (*GenBank* accession number is inside brackets after gene's name):

Agrp (AF206017): gene encoding agouti-related protein; encoded (AgRP)

5'-CGACGCGGAGAACGAGACTCGCGGTTCTGTGGATCTAGCACCTCTGCC-3'

Cartpt (M29712): gene encoding cocaine and amphetamine-regulated transcript (CART)

5'-CCGAAGGAGGCTGTCACCCCTTCACA-3'

Fasn (NM_017332): gene encoding fatty acid synthase (FAS)

5'-GGGTCCATTGTGTGTGCCTGCTTGGGGTG-3'

Npy (M20373): gene encoding neuropeptide Y (NPY)

5'-AGATGAGATGTGGGGGAAACTAGGAAAAGTCAGGAGAGCAAGTTTCATT-3'

Pomc (AF510391): gene encoding proopiomelanocortin (POMC)

5'-CTTGATGATGGCGTTCTTGAAGAGCGTCACCAGGGGCGTCTGGCTCTT-3'

Trh (NM_013046): gene encoding thyrotropin-releasing hormone (TRH)

5'-ATACCAGTTAGGGTGAAGATCAAAGCCAGAGCCAGCAGCAACCAA-3'

These probes were 3'-end labeled with ³⁵S- α dATP using terminal deoxynucleotidyl transferase (*Amersham Biosciences*). We performed in situ hybridizations as previously published ¹⁻⁶. Similar anatomical regions were analyzed using the rat brain atlas of Paxinos & Watson ⁹. The slides from all experimental groups were exposed to the same autoradiographic film. All sections were scanned and the specific hybridization signal was quantified by densitometry using a digital imaging system (*ImageJ 1.33*)¹⁻⁶. We determined the optical density of the hybridization signal and subsequently corrected by the optical density of its adjacent background value. A rectangle, with the same dimensions in each case, was drawn enclosing

the hybridization signal over each nucleus and over adjacent brain areas of each section (background). For the in situ analysis we used between 9 and 16 animals per experimental group. We used between 16 and 20 sections for each animal (4–5 slides with four sections per slide). The mean of these 16–20 values was used as the densitometry value for each animal.

Western blotting. We subjected hypothalamic total protein lysates were subjected to SDS-PAGE, electrotransferred them on a PVDF membrane and probed with the following antibodies: ACC, pACC α -Ser⁷⁹, AMPK α 1 and AMPK α 2 (*Upstate*); FAS (BD), tAMPK α , pAMPK α -Thr¹⁷², pFoxO1-Ser²⁵⁶ (*Cell Signaling*); β -actin, pSTAT3-Tyr⁷⁰⁵ (*Abcam*) as previously described^{2–6}.

Immunohistochemistry. Enzymatic immunohistochemistry (*Dako EnVision™*), immunofluorescence and double labeling were performed as described^{2,6}, using a rabbit anti-GFP (*Abcam*), rabbit anti-c-FOS (*Santa Cruz Biotechnology*), rabbit anti-pAMPK α -Thr¹⁷² (*Cell Signaling*) or goat anti-TR α (*Abcam*). We used 5–6 rats per experimental group. The specificity of Anti-pAMPK α -Thr¹⁷² antibody was shown by pre-absorption with 10 nmol ml⁻¹ of control peptide (**Supplementary Fig. 5b**). Furthermore, anti-pAMPK α -Thr¹⁷² antibody specifically detected pAMPK α when hypothalamic samples were assayed by western blot, at the expected molecular weight (62 kDa) and no additional bands were observed (**Supplementary Fig. 5c**).

Enzymatic and malonyl-CoA assays. The CPT1 activity, the AMPK α 1 and AMPK α 2 phosphotransferase activities toward the AMARA peptide and the malonyl-CoA concentration were measured as previously described^{2–6, 10}. For the AMPK α -CA and AMPK α -DN

experiments, malonyl-CoA was measured in the ventral hypothalamus, which was dissected under a microscope.

REFERENCES

1. Chakravarthy,M.V. *et al.* Brain fatty acid synthase activates PPAR-alpha to maintain energy homeostasis. *J. Clin. Invest* **117**, 2539-2552 (2007).
2. López,M. *et al.* Hypothalamic fatty acid metabolism mediates the orexigenic action of ghrelin. *Cell Metab* **7**, 389-399 (2008).
3. Vázquez,M.J. *et al.* Central resistin regulates hypothalamic and peripheral lipid metabolism in a nutritional-dependent fashion. *Endocrinology* **149**, 4534-4543 (2008).
4. Lage,R. *et al.* Ghrelin effects on neuropeptides in the rat hypothalamus depend on fatty acid metabolism actions on BSX but not on gender. *FASEB J.* **24**, 2670-2679 (2010).
5. Sangiao-Alvarellos,S. *et al.* Influence of ghrelin and GH deficiency on AMPK and hypothalamic lipid metabolism. *J. Neuroendocrinol.* **22**, 543-556 (2010).
6. López,M. *et al.* Tamoxifen-induced anorexia is associated with fatty acid synthase inhibition in the ventromedial nucleus of the hypothalamus and accumulation of malonyl-CoA. *Diabetes* **55**, 1327-1336 (2006).
7. Rahmouni,K. *et al.* Hypothalamic PI3K and MAPK differentially mediate regional sympathetic activation to insulin. *J. Clin. Invest* **114**, 652-658 (2004).
8. Nogueiras,R. *et al.* Direct control of peripheral lipid deposition by CNS GLP-1 receptor signaling is mediated by the sympathetic nervous system and blunted in diet induced obesity. *J Neurosci.* **29**, 5916-5925 (2009).
9. Paxinos,G. & Watson,C. *The rat brain in stereotaxic coordinates*(Academic Press, Sydney, 1986).
10. Lelliott,C.J. *et al.* Transcript and metabolite analysis of the effects of tamoxifen in rat liver reveals inhibition of fatty acid synthesis in the presence of hepatic steatosis. *FASEB J* **19**, 1108-1119 (2005).